



**CHALMERS**  
UNIVERSITY OF TECHNOLOGY

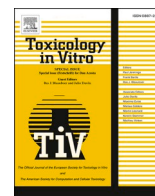
## **Animal- free skin permeation analysis using mass spectrometry imaging**

Downloaded from: <https://research.chalmers.se>, 2024-03-13 11:05 UTC

Citation for the original published paper (version of record):

Munem, M., Djuphammar, A., Sjölander, L. et al (2021). Animal- free skin permeation analysis using mass spectrometry imaging. *Toxicology in Vitro*, 71. <http://dx.doi.org/10.1016/j.tiv.2020.105062>

N.B. When citing this work, cite the original published paper.



# Animal- free skin permeation analysis using mass spectrometry imaging

Marwa Munem<sup>a,b</sup>, August Djuphammar<sup>a</sup>, Linnea Sjölander<sup>a</sup>, Lina Hagvall<sup>c</sup>, Per Malmberg<sup>a,\*</sup>

<sup>a</sup> Department of Chemistry and Chemical Engineering, Chalmers University of Technology, 412 96 Gothenburg, Sweden

<sup>b</sup> Chemistry and Molecular Biology, University of Gothenburg, 412 96 Gothenburg, Sweden

<sup>c</sup> Occupational Dermatology, Department of Clinical Sciences, Sahlgrenska Academy at the University of Gothenburg, 413 45 Gothenburg, Sweden

## ARTICLE INFO

### Keywords:

Skin permeation  
Mass spectrometry imaging  
UV-filters  
Bemotrizinol  
Biscotrizole  
Avobenzone

## ABSTRACT

Here we demonstrate an animal-free skin permeation analytical approach suitable for testing pharmaceuticals, cosmetics, occupational skin hazards and skin allergens. The method aims to replace or significantly reduce existing in-vivo models and improve on already established in-vitro models. This by offering a more sensitive and flexible analytical approach that can replace and/or complement existing methods in the OECD guidelines for skin adsorption (no 427 and no 428) and measure multiple compounds simultaneously in the skin while being able to also trace endogenous effects in cells. We demonstrate this here by studying how active ingredients in sunscreen permeate through left-over human skin, from routine surgery, in a Franz-cell permeation model. Two common sunscreens were therefore applied to the human skin and Time of flight secondary ion mass spectrometry (ToF-SIMS) was used to trace the molecules through the skin. We show that ToF-SIMS imaging can be applied in visualizing the distribution of Avobenzone, Bemotrizinol, Biscotrizole and Ethyl hexyl triazine at subcellular resolution in the skin. The UV-blockers could be visualized at the same time in one single experiment without any probes or antibodies used. The UV-blockers mostly remained in the stratum corneum. However, in certain features of the skin, such as sebaceous glands, the penetration of the UV-blockers was more prominent, and the compounds reached deeper into the epidermis.

## 1. Introduction

Human skin is the largest organ of the body with a variety of advanced functions. It protects the body from xenobiotics and microbial attacks, helps regulate body temperature and permits sensations of touch, heat and cold. Skin also functions as a barrier that regulates the penetration of various compounds. Active compound or active pharmaceutical compound, API, penetration is beneficial for drugs and some cosmetics products, while it should be prevented for other products such as UV-filters, hair dye and hygiene products. In both cases studying dermal penetration is of importance to understand the behavior of compounds that enter the human body through the skin (Karan et al., 2009). Currently the main in vitro methods to study skin penetration are a combination of vertical diffusion cells with HPLC analysis of the fluid reservoir and tape stripping (Haque et al., 2016; Martins et al., 2014; Li et al., 2015; Puglia et al., 2014). While, ICP-MS can be applied to study metal permeation in skin (Midander et al., 2020). These approaches studies how much of a compound penetrates the skin but typically does not address the distribution of the API in the skin itself. The other common problem is the choice of acceptor media, which can give false

conclusions because of solubility issues of the different APIs (Chokshi et al., 2007).

Other detection techniques that are routinely used to localize drugs in different compartments of skin are mainly imaging methods such as confocal microscopy or fluorescence measurements (Jacobi et al., 2005; Franzen et al., 2012). These techniques have the need of labeling, or are dependent on native fluorescence, which limits the number ingredients that can be detected. Those limitations can be avoided by using imaging mass spectrometry as a complementary method to HPLC.

Mass spectrometry imaging (MSI) is a label free technique which is becoming widely used to image biomolecule, drug and metal penetration in skin as well as localization in different organs (D'Alvise et al., 2014; Malmberg et al., 2018; Najafinobar et al., 2019; Zhang et al., 2020). The main advantage of MSI is the label free detection of large number of molecules within one experiment on the same tissue section allowing detection of both endogenous and exogenous compounds in parallel. Different MSI techniques have different characteristics especially when it comes to achievable lateral resolution (Bodzon-Kulakowska and Suder, 2016; Hanrieder et al., 2015) and so far Time of flight secondary ion mass spectrometry, ToF-SIMS, delivers the best possible

\* Corresponding author at: Chalmers University of Technology, Chemistry and Chemical Engineering, Kemivägen 10, 41296 Gothenburg, Sweden.

E-mail address: [malmper@chalmers.se](mailto:malmper@chalmers.se) (P. Malmberg).

<https://doi.org/10.1016/j.tiv.2020.105062>

Received 23 October 2020; Received in revised form 17 November 2020; Accepted 27 November 2020

Available online 1 December 2020

0887-2333/© 2020 The Authors. Published by Elsevier Ltd. This is an open access article under the CC BY license (<http://creativecommons.org/licenses/by/4.0/>).

lateral resolution for molecular imaging (Bodzon-Kulakowska and Suder, 2016). Previously, in the field of dermatology, imaging mass spectrometry have been applied to study follicular transport of drugs in skin using DESI (D'Alvise et al., 2014), and ToF-SIMS has been used to image basal cell carcinoma (Munem et al., 2018), age related lipid changes in stratum corneum (Starr et al., 2016), and mapping endogenous in human skin (Sjövall et al., 2018).

Compared to the more common, matrix assisted laser desorption ionization, MALDI, the use of ToF-SIMS within molecular bioimaging remains relatively limited, perhaps due to the complexity of the instrumentation and sample preparation (Nygren et al., 2006; Shon et al., 2018; Angerer et al., 2015) and sometimes the problematic fragmentation of molecular ions (Touboul et al., 2007; Passarelli and Winograd, 2011). It was previously shown that ToF-SIMS can investigate the penetration and distribution of nickel in human skin (Malmberg et al., 2018), studying skin penetration of drug substances roflumilast, tofacitinib, and ruxolitinib in mouse skin (Sjövall et al., 2014), distribution of a conventional antimicrobial compound, chlorhexidine digluconate, within porcine skin (Judd et al., 2013), and ZnO and TiO<sub>2</sub> nanoparticles penetration in pig skin (Monteiro-Riviere et al., 2011). The effect of fatty acids on the drug tolnaftate penetration into human skin was also studied by ToF-SIMS (Kezutyte et al., 2013). However, in this study we demonstrate the use of ToF-SIMS to monitor active substance penetration and localization through human skin tissue by studying sunscreen as one of many possible applications in the medical field. This method can serve as an alternative to artificial skin models and animal skin-based toxicology studies or product testing.

## 2. Materials and methods

### 2.1. Skin samples

Full-thickness human skin was obtained as excess tissue from breast reduction surgery at the Department of Plastic Surgery, Sahlgrenska University Hospital. The tissue was made anonymous upon collection in agreement with routines approved by the local ethics committee. The skin tissue was trimmed from subcutaneous fat, cut into pieces, mounted on cork sheets, wrapped in aluminum foil, and kept at  $-20^{\circ}$ . Samples were thawed at room temperature for 30 min prior to experiments. The full-thickness skin was mounted in vertical (Franz-type) skin diffusion cells (Laboratory Glass Apparatus, Berkley, CA, USA), with an exposed surface area of  $1.5\text{ cm}^2$ . Four diffusion cells were prepared. The receptor compartments were filled with 0.15 M ammonium formate (Sigma\_Aldrich, Germany). Chemical off-the-shelf sunscreens was added to diffusion cells in a thin layer, approx. 1 ml, fully covering the exposed skin surface. 2 different sunscreens were used called (sunscreen 1 and sunscreen 2, for ingredients see supplementary information Table 1). Chambers with non-exposed skin served as controls. The exposure time was 24h, and diffusion cells were kept at  $32^{\circ}\text{C}$ . On removal, sunscreen was gently removed with tissue paper and wrapped in aluminum foil and kept at  $-20^{\circ}$  prior to sectioning. In total 5 exposure experiments and 5 controls were performed.

### 2.2. Tissue preparation for ToF-SIMS

Vertical sectioning was performed using a cryostat (Leica CM1520) at  $-20^{\circ}\text{C}$  with a thickness of  $10\text{ }\mu\text{m}$  per slice. The tissue slices were then thaw mounted on a microscope slide which is conductive and transparent. No fixation was used, to avoid contamination. Hematoxylin and eosin (H & E) staining of the same sections was performed after the ToF-SIMS analysis.

### 2.3. ToF-SIMS imaging

ToF-SIMS imaging was performed with a TOF-SIMS V (ION-TOF, Münster, Germany), with a bismuth liquid metal ion gun as a primary

ion source and a C<sub>60</sub> 10-keV ion source as a sputter source. Data were recorded in positive and negative ion modes, and spectra were acquired using Bi<sub>3</sub><sup>+</sup> (25keV) primary ions. High-mass resolution images from the skin were obtained in high-current bunched mode, with a pulsed primary ion current of 0.34 pA and a maximum ion dose density of  $3 \times 10^{11}\text{ ions/cm}^2$ , that is, below the static limit. The Surface lab 6 software (v. 6.6; ION-TOF) was used for all spectrum and image recording, processing, image analysis, and 3D image analysis. The mass spectra were internally calibrated to signals of [C]<sup>+</sup>, [CH]<sup>+</sup>, [C<sub>2</sub>]<sup>+</sup>, [C<sub>3</sub>]<sup>+</sup> and [C]<sup>−</sup>, and [CH<sub>2</sub>]<sup>+</sup>, [CH<sub>3</sub>]<sup>+</sup>, and [C<sub>5</sub>H<sub>12</sub>N]<sup>+</sup>, for negative and positive ion modes, respectively. Depth profiling was performed in the non-interlaced mode with C<sub>60</sub><sup>++</sup> ions at a current of 0.180 nA, sputtering a crater of  $700 \times 700\text{ }\mu\text{m}$ , and analyzing an area of  $250 \times 250\text{ }\mu\text{m}$  with Bi<sub>3</sub><sup>+</sup> ions. The total C<sub>60</sub> dose in the experiment was  $2 \times 10^{14}\text{ ions/cm}^2$ , which corresponds to an approximate depth of 400 nm in the graft if compared with a depth profile of a standardized organic material with the same ion dose.

In total, five different experiments from sunscreen exposed samples and three controls were analyzed in different modes. The red/green/blue (RGB) color overlays are represented in a linear relationship ranging from a signal intensity of zero as black to 100% color for the maximum ion count for that respective ion.

## 3. Result and discussion

Sunscreen or sun filters are terms to describe products used to protect skin from UV light. They are usually administrated through topical routes which makes dermal penetration studies highly valuable (Gilbert et al., 2016). The chemicals that are used in these products are supposed to be photostable and remain on the skin surface. There are two types of UV-filters, physical and chemical filters. Chemical UV-filters are usually large organic molecules that have narrow absorption spectra, and thus a combination of chemical filters has to be used to cover the whole UV spectra (Serpone et al., 2007; Roelandts, 1998). Physical UV filters are mainly based on minerals such as Zinc oxide and titanium dioxide (Krause et al., 2012). Those minerals reflect the light rather than absorbing it (Sarveiya et al., 2004). Therefore they are considered to be safer than chemical filters that absorbs the UV light (Moloney et al., 2002). Skin penetration of such molecules can easily be studied by mass spectrometry imaging but has so far not been studied by ToF-SIMS.

ToF-SIMS imaging was able to image the chemical components of the sunscreens, as can be seen in Fig. 1, as well as endogenous skin substances such as fatty acids, cholesterol sulfate and phospholipids. The saturated fatty acid C24:0 ( $m/z$  367.4, Fig. 1a) can be used to distinguish the stratum corneum while cholesterol sulfate ( $m/z$  465.4, Fig. 1b), can be used as an epidermis marker (Sjövall et al., 2018). These markers together with the H&E image (Fig. 1e) were used for co-localization of the APIs in the skin tissue.

Ethylhexyloxyphenol Methoxyphenyl Triazine (Bemotrizinol) is a photostable UVB and UVA blocker. It gave a very stable signal in both positive ion mode as an  $[M + H]^+$  ion and in negative as an  $[M-H]^-$  ion at  $m/z$  628.3 and 627.3 respectively as can be seen in Fig. 1d. Another component, Methylene bis-Benzotriazolyl Tetramethyl butylphenol (Biscotrizole), a UVB and UVA sun blocker, was detected in the negative ion mode as an  $[M-H]^-$  ion, at  $m/z$  657.3, while Ethyl hexyl triazone an organic UVB filter was detected in negative ion mode as  $[M-H]^-$  ion at  $m/z$  821.3 (see supplementary information Fig. 1).

Line scans were used to compare the penetration depth of the active compounds in the skin tissue. The saturated fatty acid C24:0 was used as a reference peak for the stratum corneum. All three chemicals, Bis-Ethylhexyloxyphenol Methoxyphenyl Triazine, Methylene bis-Benzotriazolyl Tetramethyl butylphenol and Ethyl hexyl triazone were localized in the stratum corneum and hence appeared to stay on the skin surface. Fig. 2 show the Line scan measurement images of Bemotrizinol (bottom,  $m/z$  627.3) and the stratum corneum marker (top,  $m/z$  367.4) showing a similar distribution, indicating that the API remains well

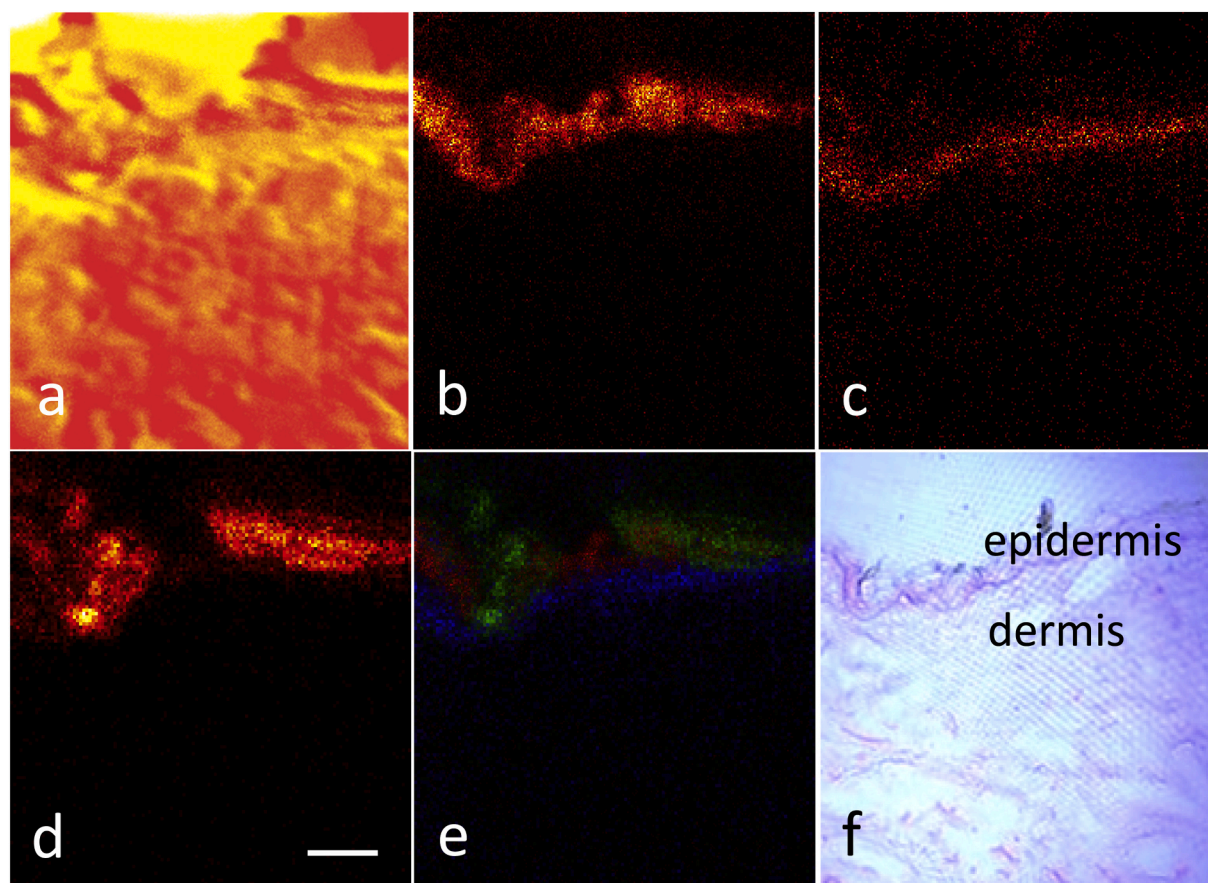


**Fig. 1.** Negative ion ToF-SIMS data of the epidermal region of skin cross section. Ion images of (from left) (a) total ion image, (b) the saturated fatty acid C24:0 ( $m/z$  367.4), (c) cholesterol sulfate ( $m/z$  465.4), (d) Bemotrizinol ( $m/z$  628.3), (e) a three color ion image of the three masses, (f) H&E image of the same tissue section corresponding to the ion images. Overlay image represent viable epidermis in blue, stratum corneum in red and the active compound in green. Field of view  $300 \times 300 \mu\text{m}$ . Scale bar  $50 \mu\text{m}$ . (For interpretation of the references to color in this figure legend, the reader is referred to the web version of this article.)

contained in the stratum corneum.

As ToF-SIMS is a very sensitive surface analytical technique only ions that are generated very close (10s of nanometers) to the surface are collected to generate a mass spectrum (Sodhi, 2004). ToF-SIMS imaging can also be performed in 3D imaging mode where depth profiling is performed by applying repeated cycles of SIMS analysis of the sample surface followed by sputter erosion that exposes a deeper layer of the sample to the next round of SIMS analysis (Breitenstein et al., 2007). In a dual-beam setup one ion beam is used to determine the chemical composition of the surface (analyzing beam, here Bismuth), and the second ion beam is only used for intermittent sputter erosion (here  $\text{C}_{60}^{++}$ ). This mode is of importance to investigate variation of the chemical composition in the depth of tissue section and also serves as a good way to clean the surface if contamination or ion suppression is suspected.

Fig. 3 is an example of a three-dimensional render of Avobenzone and Bemotrizinol distribution in skin. The ion at  $m/z$  184 was used for localization of skin tissue. It is a characteristic fragment for phosphocholine-containing lipids (Pulfer and Murphy, 2003) and is usually used for tissue localization for ToF SIMS in positive ion mode. The 2D views of this image data is shown in supplementary information Fig. 2.

Avobenzone is a very common ingredient in sunscreens and is known to be photounstable (Afonso et al., 2014). Photoallergic and cytotoxic reactions have often been associated to Avobenzone due to its photodegradation products (Schmidt et al., 1998). Previous studies on Avobenzone skin penetration show dissimilar results on Avobenzone penetration based on different test animals. For example, studies of Avobenzone penetration in pig ear using HPLC show no penetration,

while other studies showed appreciable amounts of Avobenzone in the receiving phase through rat skin, and nude mice skin using the same technique (Haque et al., 2016; Tampucci et al., 2018). Here, Avobenzone, was detected in both positive and negative ion mode at  $m/z$  311.1 and  $m/z$  310.1. Conventional 2D-imaging experiments gave only a weak intensity of the peak in the generated spectra and in the resulting ion images. This can be caused of an overlap with endogenous peaks from the skin surface that are removed during the 3D-imaging sputter (dig-through process). Another explanation could be ion suppression caused by surface abundant lipid species (Angerer et al., 2015).

The transport of chemicals through human skin is a complex process. There are three major mechanisms by which skin absorption may occur. Transcellular absorption where the chemical travels through the cell membrane of the keratin-packed corneocytes. The second pathway – intercellular absorption occurs when the chemical is transferred around the corneocytes in the lipid-rich extracellular regions. Appendageal absorption is the process when the chemical bypasses the corneocytes, and enters the shunts provided by the hair follicles, sweat glands, and sebaceous glands. The last mentioned mechanism plays big role in areas that are rich with hair follicles and sebaceous gland can work as a reservoir for the chemical. (Wilkinson, 2008) We therefore studied a sebaceous gland in more detail as can be seen in Fig. 4. The ion image of Avobenzone was compared to the H&E image (Fig. 4) of the same section to confirm sebaceous gland's anatomical structure in the ion image. The ion image was also compared to cholesterol sulfate ion image. A line scan was also performed for both ion images (see supplementary information Fig. 3). Avobenzone here penetrates to the viable dermis which is supported by the literature.



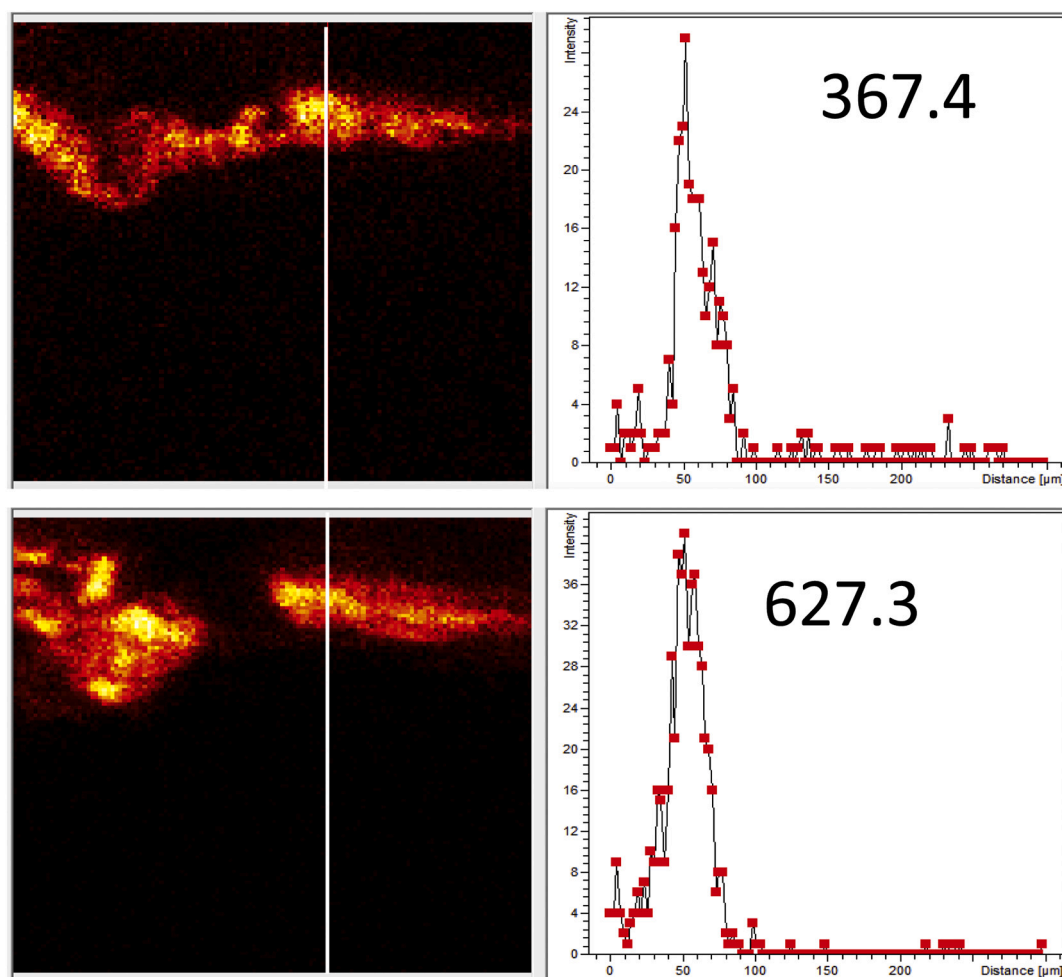


**Fig. 2.** Line scan images of Bemotrizinol ( $m/z$  627.3) and C:24 stratum corneum marker ( $m/z$  367.4) distribution on the same region on skin. Images reveal that Bemotrizinol have same distribution as C24:0 i.e. it stays in the skin surface.

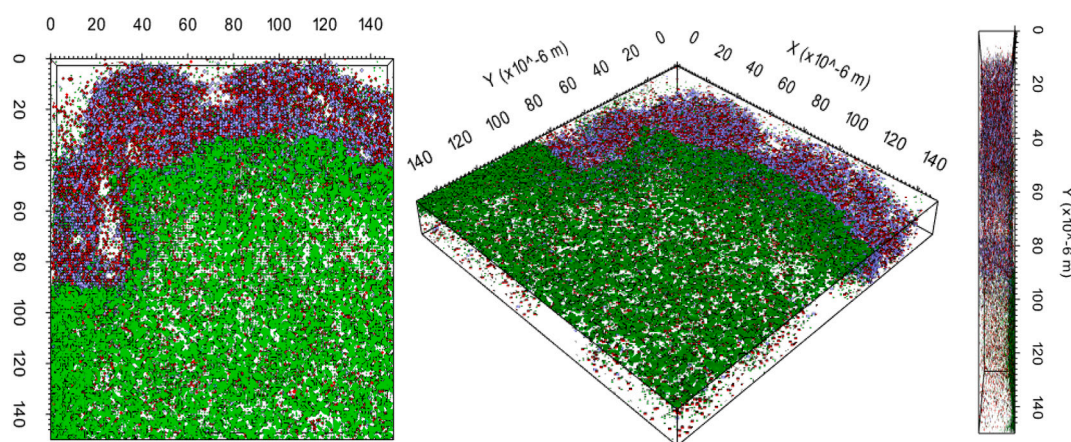


**Fig. 3.** Different views of three-dimensional render of Bemotrizinol (in purple) and Avobenzone (in red) distribution on skin tissue (green). Field of view 150x150  $\mu\text{m}$ . (For interpretation of the references to color in this figure legend, the reader is referred to the web version of this article.)

Follicular transport is a known route as confirmed by many in vivo and invitro studies (D'Alvise et al., 2014) (Samuelsson et al., 2009; Otberg et al., 2008; Trauer et al., 2009). It has been shown that follicles with their associated sebaceous glands penetrate the skin barrier and they bypass the bulk epidermis, as referred to the shunt path (Essa et al., 2002). The hair follicle, hair shaft, and sebaceous gland together also

form the so called pilosebaceous unit. Since sebaceous glands are associated with the hair follicles secrete sebum (Lauer et al., 1995), Avobenzone is able to penetrate skin through appendageal transport. More specifically through follicular transport and the sebaceous gland act as the reservoir.

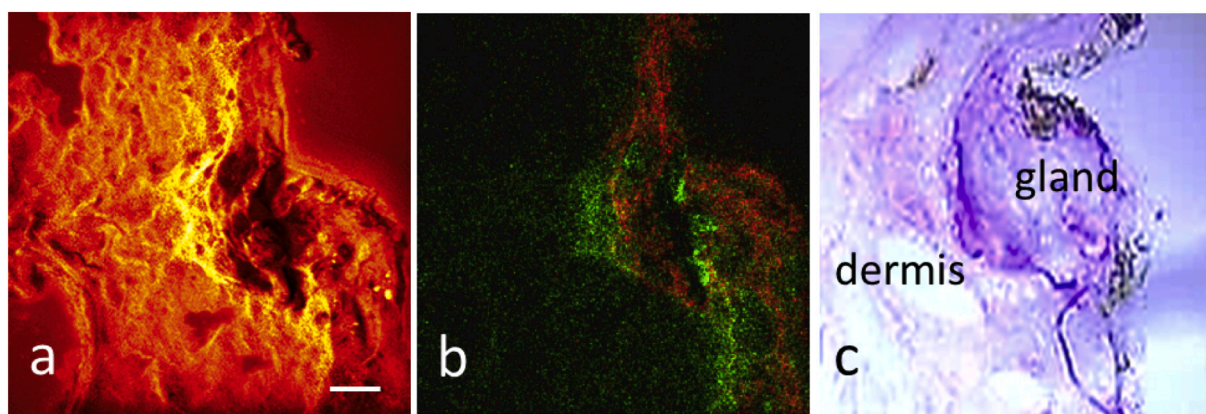


**Fig. 4.** Negative ion ToF-SIMS data of the epidermal region of skin cross section. Ion images of (from left), (a) total ion image of the region, (b) two-color ion image of Avobenzone (green) and the fatty acid C24:0 (red) and (c) H&E image of the same Area. Field of view  $250 \times 250 \mu\text{m}$ . Scale bar  $20 \mu\text{m}$ . (For interpretation of the references to color in this figure legend, the reader is referred to the web version of this article.)

### 3.1. Skin permeability

It is well known that there are considerable differences between animal and humans in their skin delivery systems, attributed to factors including stratum corneum thickness, hydration, and lipid composition (Barbero and Frisch, 2009). Using fresh frozen human skin instead of animal skin can serve as an excellent alternative to methods using animal skin while also making the result much closer to human living skin. Although the tissue has been frozen and stored at  $-80^\circ\text{C}$ , transport and barrier mechanisms apparently remain functional as shown earlier (Malmberg et al., 2018). Similar distributions patterns has also been demonstrated by others in porcine skin (Herbig et al., 2015). While the experiments there were performed with skin kept at  $-80^\circ\text{C}$ , freeze thaw cycles or careless storage at higher temperatures might affect the results and the permeability of the skin.

No apparent differences between the 2 sunscreens tested (sunscreens 1 and sunscreen 2) could be detected here. The 2 sunscreens have similar active ingredients, but the concentration is not disclosed by the manufacturers. A more in-depth study would be needed to evaluate any differences caused by other ingredients. It is worth mentioning that the same experiment has been replicated on the same tissue after more than 6 months. As expected, the skin permeability changed, and all APIs showed higher penetration down to the dermis. The distribution of the chemicals showed a higher degree of variation (see supplementary information Fig. 4). Avobenzone showed a similar distribution to Fig. 3 and showed its maximum concentration in the stratum corneum. However, it also showed a higher level of permeation into the dermis. The same could be said for Bemotrizinol and Biscotrizole that while showing a strong signal from the stratum corneum, also penetrated into the dermis. The signals accumulated as dotted structures that could be attributed to fat deposits inside the skin as correlated by the ion signal for diacylglycerols. Further studies are needed to understand how exactly the skin changes in long term-storage and how it could affect skin permeation in this model.

## 4. Conclusions

ToF-SIMS imaging is an informative technique for analyzing the penetration of different chemicals in the skin. It provides the ability to analyze the distribution of several selected compounds simultaneously without a prior knowledge about the chemical, which eliminates the need of any labelling or extraction step that is essential for most analytical techniques. The current study showed that TOF-SIMS imaging can be applied in visualizing the distribution of Avobenzone, Bemotrizinol, Biscotrizole and Ethyl hexyl triazine, that are commonly used in sunscreen formulations. The compounds showed different abilities to

penetrate the skin depending on their structure and physicochemical properties but in general remained in the stratum corneum. An exception could be seen with Avobenzone which penetrated into the dermis through a sebaceous gland. Similar results have been reported in the literature using other techniques (Haque et al., 2016; Mavon et al., 2007) indicating that the model can be used to study skin permeation of active pharmaceutical compounds and other chemical compounds. The model needs to be further validated but can be said to give accurate result. Ethically, it is an excellent way to avoid using experimental animals and could be considered as alternative method for the currently used methods in permeation studies.

### Declaration of Competing Interest

The authors declare that they have no known competing financial interests or personal relationships that could have appeared to influence the work reported in this paper.

### Acknowledgements

We gratefully acknowledge support from Forska Utan Djurförsök and Hudfonden (N2019-0001) to "Forska utan Djurförsök".

### Appendix A. Supplementary data

Supplementary data to this article can be found online at <https://doi.org/10.1016/j.tiv.2020.105062>.

### References

- Afonso, S., Horita, K., Sousa e Silva, J.P., Almeida, I.F., Amaral, M.H., Lobão, P.A., Costa, P.C., Miranda, M.S., Esteves da Silva, J.C.G., Sousa Lobo, J.M., 2014. Photodegradation of Avobenzone: Stabilization Effect of Antioxidants. *J. Photochem. Photobiol. B* 140, 36–40. <https://doi.org/10.1016/j.jphotobiol.2014.07.004>.
- Angerer, T.B., Dowlathshahi Pour, M., Malmberg, P., Fletcher, J.S., 2015. Improved molecular imaging in rodent brain with time-of-flight-secondary ion mass spectrometry using gas cluster ion beams and reactive vapor exposure. *Anal. Chem.* 87 (8), 4305–4313. <https://doi.org/10.1021/ac504774y>.
- Barbero, A.M., Frisch, H.F., 2009. Pig and guinea pig skin as surrogates for human in vitro penetration studies: a quantitative review. *Toxicol. in Vitro* 23 (1), 1–13. <https://doi.org/10.1016/j.tiv.2008.10.008>.
- Bodzon-Kulakowska, A., Suder, P., 2016. Imaging mass spectrometry: instrumentation, applications, and combination with other visualization techniques. *Mass Spectrom. Rev.* 35 (1), 147–169. <https://doi.org/10.1002/mas.21468>.
- Breitenstein, D., Rommel, C.E., Möllers, R., Wegener, J., Hagenhoff, B., 2007. The chemical composition of animal cells and their intracellular compartments reconstructed from 3D mass spectrometry. *Angew. Chem. Int. Ed.* 46 (28), 5332–5335. <https://doi.org/10.1002/anie.200604468>.
- Chokshi, R.J., Zia, H., Sandhu, H.K., Shah, N.H., Mallick, W.A., 2007. Improving the dissolution rate of poorly water soluble drug by solid dispersion and solid

- solution—pros and cons. *Drug Deliv.* 14 (1), 33–45. <https://doi.org/10.1080/10717540600640278>.
- D'Alvise, J., Mortensen, R., Hansen, S.H., Janfelt, C., 2014. Detection of follicular transport of lidocaine and metabolism in adipose tissue in pig ear skin by DESI mass spectrometry imaging. *Anal. Bioanal. Chem.* 406 (15), 3735–3742. <https://doi.org/10.1007/s00216-014-7802-z>.
- Essa, E.A., Bonner, M.C., Barry, B.W., 2002. Human skin sandwich for assessing shunt route penetration during passive and iontophoretic drug and liposome delivery. *J. Pharm. Pharmacol.* 54 (11), 1481–1490. <https://doi.org/10.1211/002235702135>.
- Franzen, L., Mathes, C., Hansen, S., Windbergs, M., 2012. Advanced chemical imaging and comparison of human and porcine hair follicles for drug delivery by confocal Raman microscopy. *J. Biomed. Opt.* 18 (6), 061210.
- Gilbert, E., Roussel, L., Serre, C., Sandouk, R., Salmon, D., Kirilov, P., Haftek, M., Falson, F., Pirot, F., 2016. Percutaneous absorption of benzophenone-3 loaded lipid nanoparticles and polymeric nanocapsules: a comparative study. *Int. J. Pharm.* 504 (1–2), 48–58. <https://doi.org/10.1016/j.ijpharm.2016.03.018>.
- Hanrieder, J., Malmberg, P., Ewing, A.G., 2015. Spatial neuroproteomics using imaging mass spectrometry. *Biochim. Biophys. Acta* 1854 (7), 718–731. <https://doi.org/10.1016/j.bbapap.2014.12.026>.
- Haq, T., Crowther, J.M., Lane, M.E., Moore, D.J., 2016. Chemical ultraviolet absorbers topically applied in a skin barrier mimetic formulation remain in the outer stratum corneum of porcine skin. *Int. J. Pharm.* 510 (1), 250–254. <https://doi.org/10.1016/j.ijpharm.2016.06.041>.
- Herbig, M.E., Houdek, P., Gorissen, S., Zorn-Kruppa, M., Wladykowski, E., Volksdorf, T., Grzybowski, S., Kolios, G., Willers, C., Mallwitz, H., Moll, I., Brandner, J.M., 2015. A custom tailored model to investigate skin penetration in porcine skin and its comparison with human skin. *Eur. J. Pharm. Biopharm.* 95, 99–109. <https://doi.org/10.1016/j.ejpb.2015.03.030>.
- Jacobi, U., Toll, R., Sterry, W., Lademann, J., 2005. Do follicles play a role as penetration pathways in *in vitro* studies on porcine skin?—an optical study. *Laser Phys.* 15 (11), 1594–1598.
- Judd, A.M., Scurr, D.J., Heylings, J.R., Wan, K.-W., Moss, G.P., 2013. Distribution and visualisation of chlorhexidine within the skin using ToF-SIMS: a potential platform for the design of more efficacious skin antiseptic formulations. *Pharm. Res.* 30 (7), 1896–1905. <https://doi.org/10.1007/s11095-013-1032-5>.
- Karan, A., Alikhan, A., Maibach, H.I., 2009. Toxicologic implications of cutaneous barriers: a molecular, cellular, and anatomical overview. *J. Appl. Toxicol.* 29 (7), 551–559. <https://doi.org/10.1002/jat.1461>.
- Kezutye, T., Desbenoit, N., Brunelle, A., Briedis, V., 2013. Studying the penetration of fatty acids into human skin by *ex vivo* ToF-SIMS imaging. *Biointerphases* 8 (1), 3. <https://doi.org/10.1186/1559-4106-8-3>.
- Krause, M., Klit, A., Jensen, M.B., Søborg, T., Frederiksen, H., Schlumpf, M., Lichtensteiger, W., Skakkebaek, N.E., Drzewiecki, K.T., 2012. Sunscreens: are they beneficial for health? An overview of endocrine disrupting properties of UV-filters. *Int. J. Androl.* 35 (3), 424–436. <https://doi.org/10.1111/j.1365-2605.2012.01280.x>.
- Lauer, A.C., Lieb, L.M., Ramachandran, C., Flynn, G.L., Weiner, N.D., 1995. Transfollicular drug delivery. *Pharm. Res.* 12 (2), 179–186. <https://doi.org/10.1023/a:1016250422596>.
- Li, C.C., Lin, Y.T., Chen, Y.T., Sie, S.F., Chen-Yang, Y.W., 2015. Improvement in UV protection retention capability and reduction in skin penetration of benzophenone-3 with mesoporous silica as drug carrier by encapsulation. *J. Photochem. Photobiol. B* 148, 277–283. <https://doi.org/10.1016/j.jphotobiol.2015.04.027>.
- Malmberg, P., Guttenberg, T., Ericson, M.B., Hagvall, L., 2018. Imaging mass spectrometry for novel insights into contact allergy – a proof-of-concept study on nickel. *Contact Dermatitis* 78 (2), 109–116. <https://doi.org/10.1111/cod.12911>.
- Martins, R.M., Siqueira, S., Fonseca, M.J.V., Freitas, L.A.P., 2014. Skin penetration and photoprotection of topical formulations containing benzophenone-3 solid lipid microparticles prepared by the solvent-free spray-congealing technique. *J. Microencapsul.* 31 (7), 644–653. <https://doi.org/10.3109/02652048.2014.911378>.
- Mavon, A., Miquel, C., Lejeune, O., Payre, B., Moretto, P., 2007. *In vitro* percutaneous absorption and *in vivo* stratum corneum distribution of an organic and a mineral sunscreen. *Skin Pharmacol. Physiol.* 20 (1), 10–20. <https://doi.org/10.1159/000096167>.
- Midander, K., Schenk, L., Julander, A., 2020. A novel approach to monitor skin permeation of metals *in vitro*. *Regul. Toxicol. Pharmacol.* 115, 104693. <https://doi.org/10.1016/j.yrtph.2020.104693>.
- Moloney, F.J., Collins, S., Murphy, G.M., 2002. Sunscreens. *Am. J. Clin. Dermatol.* 3 (3), 185–191. <https://doi.org/10.2165/00128071-200203030-00005>.
- Monteiro-Riviere, N.A., Wiench, K., Landsiedel, R., Schulte, S., Inman, A.O., Riviere, J.E., 2011. Safety evaluation of sunscreen formulations containing titanium dioxide and zinc oxide nanoparticles in UVB sunburned skin: an *in vitro* and *in vivo* study. *Toxicol. Sci. Off. J. Soc. Toxicol.* 123 (1), 264–280. <https://doi.org/10.1093/toxsci/kfr148>.
- Munem, M., Zaar, O., Dimovska Nilsson, K., Neittaanmäki, N., Paoli, J., Fletcher, J.S., 2018. Chemical imaging of aggressive basal cell carcinoma using time-of-flight secondary ion mass spectrometry. *Biointerphases* 13 (3), 03B402. <https://doi.org/10.1116/1.5016254>.
- Najafinobar, N., Venkatesan, S., von Sydow, L., Klarqvist, M., Olsson, H., Zhou, X.-H., Cloonan, S.M., Malmberg, P., 2019. ToF-SIMS mediated analysis of human lung tissue reveals increased iron deposition in COPD (GOLD IV) patients. *Sci. Rep.* 9 (1), 1–9. <https://doi.org/10.1038/s41598-019-46471-7>.
- Nygren, H., Borner, K., Malmberg, P., Hagenhoff, B., 2006. Localization of cholesterol in rat cerebellum with imaging ToF-SIMS - effect of tissue preparation. *Appl. Surf. Sci.* 252 (19), 6975–6981. <https://doi.org/10.1016/j.apsusc.2006.02.197>.
- Otberg, N., Patzelt, A., Rasulev, U., Hagemester, T., Linscheid, M., Sinkgraven, R., Sterry, W., Lademann, J., 2008. The role of hair follicles in the percutaneous absorption of caffeine. *Br. J. Clin. Pharmacol.* 65 (4), 488–492. <https://doi.org/10.1111/j.1365-2125.2007.03065.x>.
- Passarelli, M.K., Winograd, N., 2011. Characterizing *in situ* glycerophospholipids with SIMS and MALDI methodologies. *Surf. Interface Anal.* 43 (1–2), 269–271. <https://doi.org/10.1002/sia.3529>.
- Puglia, C., Damiani, E., Offerta, A., Rizza, L., Tirendi, G.G., Tarico, M.S., Curreri, S., Bonina, F., Perrotta, R.E., 2014. Evaluation of nanostructured lipid carriers (NLC) and nanoemulsions as carriers for UV-filters: characterization, *in vitro* penetration and photostability studies. *Eur. J. Pharm. Sci. Off. J. Eur. Fed. Pharm. Sci.* 51, 211–217. <https://doi.org/10.1016/j.ejps.2013.09.023>.
- Pulfer, M., Murphy, R.C., 2003. Electrospray mass spectrometry of phospholipids. *Mass Spectrom. Rev.* 22 (5), 332–364. <https://doi.org/10.1002/mas.10061>.
- Roelands, 1998. Shedding light on sunscreens. *Clin. Exp. Dermatol.* 23 (4), 147–157. <https://doi.org/10.1046/j.1365-2230.1998.00353.x>.
- Samuelsson, K., Simonsson, C., Jonsson, C.A., Westman, G., Ericson, M.B., Karlberg, A.-T., 2009. Accumulation of FITC near stratum corneum—visualizing epidermal distribution of a strong sensitizer using two-photon microscopy. *Contact Dermatitis* 61 (2), 91–100. <https://doi.org/10.1111/j.1600-0536.2009.01591.x>.
- Sarveiya, V., Risk, S., Benson, H.A.E., 2004. Liquid chromatographic assay for common sunscreen agents: application to *in vivo* assessment of skin penetration and systemic absorption in human volunteers. *J. Chromatogr. B* 803 (2), 225–231. <https://doi.org/10.1016/j.jchromb.2003.12.022>.
- Schmidt, T., Ring, J., Abeck, D., 1998. Photoallergic contact dermatitis due to combined UVB (4-Methylbenzylidene camphor/Octyl Methoxycinnamate) and UVA (Benzophenone-3/butyl Methoxydibenzoylmethane) absorber sensitization. *Dermatol. Basel Switz.* 196 (3), 354–357. <https://doi.org/10.1159/000017915>.
- Serpone, N., Dondi, D., Albini, A., 2007. Inorganic and organic UV filters: their role and efficacy in sunscreens and sun care products. *Inorg. Chim. Acta* 360 (3), 794–802.
- Shon, H.K., Kim, S.H., Yoon, S., Shin, C.Y., Lee, T.G., 2018. Molecular depth profiling on rat brain tissue sections prepared using different sampling methods. *Biointerphases* 13 (3), 03B411. <https://doi.org/10.1116/1.5019611>.
- Sjövall, P., Greve, T.M., Clausen, S.K., Møller, K., Eirefelt, S., Johansson, B., Nielsen, K.T., 2014. Imaging of distribution of topically applied drug molecules in mouse skin by combination of time-of-flight secondary ion mass spectrometry and scanning electron microscopy. *Anal. Chem.* 86 (7), 3443–3452.
- Sjövall, P., Skedung, L., Gregoire, S., Biganska, O., Clément, F., Luengo, G.S., 2018. Imaging the distribution of skin lipids and topically applied compounds in human skin using mass spectrometry. *Sci. Rep.* 8 (1), 1–14. <https://doi.org/10.1038/s41598-018-34286-x>.
- Sodhi, R.N., 2004. Time-of-flight secondary ion mass spectrometry (TOF-SIMS):—versatility in chemical and imaging surface analysis. *Analyst* 129 (6), 483–487. <https://doi.org/10.1039/B402607C>.
- Starr, N.J., Johnson, D.J., Wibawa, J., Marlow, I., Bell, M., Barrett, D.A., Scurr, D.J., 2016. Age-related changes to human stratum corneum lipids detected using time-of-flight secondary ion mass spectrometry following *in vivo* sampling. *Anal. Chem.* 88 (8), 4400–4408. <https://doi.org/10.1021/acs.analchem.5b04872>.
- Tampucci, S., Burgalassi, S., Chetoni, P., Monti, D., 2018. Cutaneous permeation and penetration of sunscreens: formulation strategies and *in vitro* methods. *Cosmetics* 5 (1), 1. <https://doi.org/10.3390/cosmetics5010001>.
- Touboul, D., Roy, S., Germain, D.P., Chaminade, P., Brunelle, A., Laprévotte, O., 2007. MALDI-TOF and cluster-TOF-SIMS imaging of fabry disease biomarkers. *Int. J. Mass Spectrom.* 260 (2–3), 158–165. <https://doi.org/10.1016/j.ijms.2006.09.027>.
- Trauer, S., Patzelt, A., Otberg, N., Knorr, F., Rozycki, C., Balizs, G., Büttmeyer, R., Linscheid, M., Liebsch, M., Lademann, J., 2009. Permeation of topically applied caffeine through human skin – a comparison of *in vivo* and *in vitro* data. *Br. J. Clin. Pharmacol.* 68 (2), 181–186. <https://doi.org/10.1111/j.1365-2125.2009.03463.x>.
- Wilkinson, S.C., 2008. Skin as a Route of Entry. In: *Principles and Practice of Skin Toxicology*. John Wiley & Sons, Ltd 69–82. <https://doi.org/10.1002/9780470773093.ch4>. <https://onlinelibrary.wiley.com/doi/10.1002/9780470773093.ch4>.
- Zhang, D., Bian, Q., Zhou, Y., Huang, Q., Gao, J., 2020. The application of label-free imaging technologies in transdermal research for deeper mechanism revealing. *Asian J. Pharm. Sci.* <https://doi.org/10.1016/j.ajps.2020.07.004>.